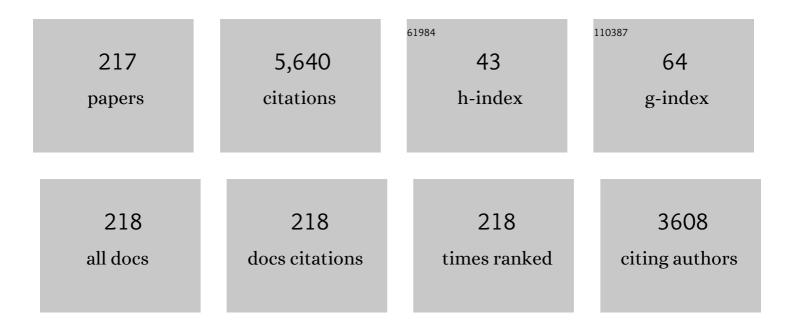
Chi Chiu Chan

List of Publications by Year in descending order

Source: https://exaly.com/author-pdf/4607606/publications.pdf Version: 2024-02-01



Сні Сніц Снам

#	Article	IF	CITATIONS
1	Enhanced Sensitivity Refractometer Based on Spherical Mach–Zehnder Interferometer With Side-Polished Structure. IEEE Sensors Journal, 2021, 21, 1548-1553.	4.7	15
2	Fiber Bragg Grating Sensors for Clinical Measurement of the First Metatarsophalangeal Joint Quasi-Stiffness. IEEE Sensors Journal, 2020, 20, 1322-1328.	4.7	10
3	Test-retest reliability of a clinical foot assessment device for measuring first metatarsophalangeal joint quasi-stiffness. Foot, 2020, 45, 101742.	1.1	6
4	VALIDITY OF A FBG-BASED SMART SOCK SYSTEM FOR MEASURING TOE GRIP FUNCTION IN HUMAN FOOT. Journal of Mechanics in Medicine and Biology, 2020, 20, 2050015.	0.7	2
5	Optical Fiber Copper (II) ion Sensor Based on Long Period Fiber Grating. , 2020, , .		2
6	Evaluating On-Water Kayak Paddling Performance Using Optical Fiber Technology. IEEE Sensors Journal, 2019, 19, 11918-11925.	4.7	12
7	Polypyrrole-Coated Polarization Maintaining Fiber-Based Vernier Effect for Isopropanol Measurement. Journal of Lightwave Technology, 2019, 37, 2768-2772.	4.6	12
8	Chitosan/Poly (Acrylic Acid) Based Fiber-Optic Surface Plasmon Resonance Sensor for Cu ²⁺ Ions Detection. Journal of Lightwave Technology, 2019, 37, 2246-2252.	4.6	30
9	Reflection-Based Thin-Core Modal Interferometry Optical Fiber Functionalized With PAA-PBA/PVA for Glucose Detection Under Physiological pH. Journal of Lightwave Technology, 2019, 37, 2773-2777.	4.6	7
10	Ion-Imprinted Chitosan-Based Interferometric Sensor for Selective Detection of Heavy Metal Ions. Journal of Lightwave Technology, 2019, 37, 2778-2783.	4.6	18
11	Carbon-nanotube / Polyvinyl alcohol coated thin core fiber sensor for humidity measurement. Sensors and Actuators B: Chemical, 2018, 257, 800-806.	7.8	56
12	Chitosan-nickel film based interferometric optical fiber sensor for label-free detection of histidine tagged proteins. Biosensors and Bioelectronics, 2018, 99, 578-585.	10.1	30
13	Kayaking paddle blade compression load distribution sensing system based on optical fiber with a polydimethylsiloxane membrane. Applied Optics, 2018, 57, 1387.	1.8	4
14	Fiber Optic Fabry–Perot Optofluidic Sensor With a Focused Ion Beam Ablated Microslot For Fast Refractive Index and Magnetic Field Measurement. IEEE Journal of Selected Topics in Quantum Electronics, 2017, 23, 322-326.	2.9	40
15	Fiber optic nickel ion sensor based on direct ligand immobilization. Proceedings of SPIE, 2017, , .	0.8	0
16	Localized surface plasmon resonance refractometer based on no-core fiber. , 2017, , .		2
17	An Ultrahigh Sensitivity Point Temperature Sensor Based on Fiber Loop Mirror. IEEE Journal of Selected Topics in Quantum Electronics, 2017, 23, 274-277.	2.9	9
18	A chitosan-coated humidity sensor based on Mach-Zehnder interferometer with waist-enlarged fusion bitapers. Optical Fiber Technology, 2017, 33, 56-59.	2.7	50

#	Article	IF	CITATIONS
19	Miniature pH sensor based on thin-core fiber Mach-Zehnder interferometer. , 2017, , .		Ο
20	Detection of Ni ²⁺ with optical fiber Mach-Zehnder interferometer coated with chitosan/MWCNT/PAA. , 2017, , .		2
21	Miniature optical fiber sensor based on polypyrrole for detection of VOCs. , 2017, , .		Ο
22	Sensitivity dependence of fiber loop mirror on the length of high birefringence fiber. Sensors and Actuators A: Physical, 2016, 247, 393-396.	4.1	3
23	Heavy Metal Cation Probe with Signal to Noise Ratio Measurement of Fiber Bragg Grating. Procedia Engineering, 2016, 140, 67-71.	1.2	4
24	Chitosan/PAA based fiber-optic interferometric sensor for heavy metal ions detection. Sensors and Actuators B: Chemical, 2016, 233, 31-38.	7.8	74
25	In-fiber Photo-immobilization of Bioactive Surfaces: An Optimization Study. Procedia Engineering, 2016, 140, 166-170.	1.2	0
26	PDMS-coated fiber volatile organic compounds sensors. Applied Optics, 2016, 55, 3543.	2.1	42
27	Miniature pH Optical Fiber Sensor Based on Fabry–Perot Interferometer. IEEE Journal of Selected Topics in Quantum Electronics, 2016, 22, 331-335.	2.9	49
28	Heavy metal ions probe with relative measurement of fiber Bragg grating. Sensors and Actuators B: Chemical, 2016, 230, 353-358.	7.8	23
29	Fluorospectroscopy of Dye-Loaded Liposomes in Photonic Crystal Fibers. IEEE Journal of Selected Topics in Quantum Electronics, 2016, 22, 21-26.	2.9	2
30	Zeolite thin film-coated spherical end-face fiber sensors for detection of trace organic vapors. Optics Communications, 2016, 364, 55-59.	2.1	21
31	Chitosan-hydrogel-based fiber optic sensor for heavy metal ion detection. Proceedings of SPIE, 2015, , .	0.8	Ο
32	Optical fiber Fabry-Perot interferometer with pH sensitive hydrogel film for hazardous gases sensing. , 2015, , .		1
33	Photonic crystal fiber interferometric pH sensor based on polyvinyl alcohol/polyacrylic acid hydrogel coating. Applied Optics, 2015, 54, 2647.	1.8	55
34	Miniature temperature sensor with germania-core optical fiber. Optics Express, 2015, 23, 17687.	3.4	19
35	Intensity-modulated relative humidity sensing with polyvinyl alcohol coating and optical fiber gratings. Applied Optics, 2015, 54, 2620.	1.8	23
36	Graphene-deposited photonic crystal fibers for continuous refractive index sensing applications. Optics Express, 2015, 23, 31286.	3.4	28

#	Article	IF	CITATIONS
37	Optical fiber magnetic field sensor based on magnetic fluid and microfiber mode interferometer. Optics Communications, 2015, 336, 5-8.	2.1	80
38	Magnetic Field Sensing With Reflectivity Ratio Measurement of Fiber Bragg Grating. IEEE Sensors Journal, 2015, 15, 1372-1376.	4.7	28
39	Relative humidity sensor based on optical fiber gratings and polyvinyl alcohol. , 2014, , .		4
40	Miniature pH sensor based on optical fiber Fabry-Perot interferometer. , 2014, , .		3
41	Magnetic field sensor based on reflection spectrum measurement of fiber Bragg grating. Proceedings of SPIE, 2014, , .	0.8	0
42	Photonic Crystal Fiber Loop Mirror-Based Chemical Vapor Sensor. Journal of Lightwave Technology, 2014, 32, 4416-4421.	4.6	8
43	In-fiber fluorospectroscopy based on a spectral decomposition method. Optics Express, 2014, 22, 23640.	3.4	5
44	In-fiber photo-immobilization of a bioactive surface. Journal of Biomedical Optics, 2014, 19, 120502.	2.6	5
45	Double-pass Mach–Zehnder fiber interferometer pH sensor. Journal of Biomedical Optics, 2014, 19, 047002.	2.6	15
46	Sensitivity-enhanced Michelson interferometric humidity sensor with waist-enlarged fiber bitaper. Sensors and Actuators B: Chemical, 2014, 194, 180-184.	7.8	92
47	Enhancement of the sensitivity of magneto-optical fiber sensor by magnifying the birefringence of magnetic fluid film with Loyt-Sagnac interferometer. Sensors and Actuators B: Chemical, 2014, 191, 19-23.	7.8	97
48	Miniature pH optical fiber sensor based on waist-enlarged bitaper and mode excitation. Sensors and Actuators B: Chemical, 2014, 191, 579-585.	7.8	29
49	Two-Phase Photobleaching Dequenching in Dye-Loaded Liposomes. IEEE Journal of Selected Topics in Quantum Electronics, 2014, 20, 213-220.	2.9	3
50	A fiber-optic pH sensor based on polyelectrolyte multilayers embedded with gold nanoparticles. Measurement Science and Technology, 2014, 25, 075102.	2.6	4
51	Continuous refractive index sensing based on carbon-nanotube-deposited photonic crystal fibers. Sensors and Actuators B: Chemical, 2014, 202, 1097-1102.	7.8	24
52	Poly(vinyl alcohol) hydrogel based fiber interferometer sensor for heavy metal cations. Sensors and Actuators B: Chemical, 2014, 202, 185-193.	7.8	45
53	Fiber Optic Refractometer Based on Cladding Excitation of Localized Surface Plasmon Resonance. IEEE Photonics Technology Letters, 2013, 25, 556-559.	2.5	26
54	Lab-in-fiber platform for plasmonic photothermal study. Proceedings of SPIE, 2013, , .	0.8	0

#	Article	IF	CITATIONS
55	Multi-layered liposomes as optical resonators. , 2013, , .		1
56	Temperature-independent accelerometer using a fiber Bragg grating incorporating a biconical taper. Optical Fiber Technology, 2013, 19, 410-413.	2.7	10
57	Magneto-optical fiber sensor based on magnetic fluid surrounded tilted fiber Bragg grating. , 2013, , .		1
58	Humidity Sensor With a PVA-Coated Photonic Crystal Fiber Interferometer. IEEE Sensors Journal, 2013, 13, 2214-2216.	4.7	85
59	Label-free fiber-optic interferometric immunosensors based on waist-enlarged fusion taper. Sensors and Actuators B: Chemical, 2013, 178, 176-184.	7.8	37
60	Fabry–Perot fiber-optic immunosensor based on suspended layer-by-layer (chitosan/polystyrene) Tj ETQq0 0 0	rgBT/Ove 7.8	erlogg 10 Tf 50
61	Temperature-independent refractometer based on a tapered photonic crystal fiber interferometer. Optics Communications, 2013, 291, 238-241.	2.1	17
62	Photonic Crystal Fiber Surface Plasmon Resonance Biosensor Based on Protein G Immobilization. IEEE Journal of Selected Topics in Quantum Electronics, 2013, 19, 4602107-4602107.	2.9	51
63	Simultaneous measurement of relative humidity and temperature with PCF-MZI cascaded by fiber Bragg grating. Optics Communications, 2013, 303, 42-45.	2.1	59
64	Miniature refractometer based on Mach–Zehnder interferometer with waist-enlarged fusion bitaper. Optics Communications, 2013, 292, 84-86.	2.1	35
65	A compact opto-fluidic platform for chemical sensing with photonic crystal fibers. Sensors and Actuators A: Physical, 2013, 191, 22-26.	4.1	9
66	Laser self-induced tunable birefringence of magnetic fluid. Applied Physics Letters, 2013, 102, .	3.3	10
67	Magnetic field sensor using tilted fiber grating interacting with magnetic fluid. Optics Express, 2013, 21, 17863.	3.4	93
68	Simultaneous Measurement of Strain and Temperature with Hollow Core Fiber Based Intermodal Interferometer. Applied Mechanics and Materials, 2013, 330, 231-236.	0.2	0
69	Optical fiber humidity sensor based on Michelson interferometric structures. , 2013, , .		3
70	Temperature Sensor Based on Modal Interference in Hollow-Core Photonic Bandgap Fiber With Collapse Splicing. IEEE Sensors Journal, 2012, 12, 1421-1424.	4.7	12
71	Tilted Long Period Gratings Pressure Sensing in Solid Core Photonic Crystal Fibers. IEEE Sensors Journal, 2012, 12, 954-957.	4.7	9
72	Sensitivity characteristics of high-birefringence Sagnac interferometer sensors. , 2012, , .		0

#	Article	IF	CITATIONS
73	Miniature photonic crystal optical fiber humidity sensor based on polyvinyl alcohol. , 2012, , .		1
74	High Extinction Ratio Magneto-Optical Fiber Modulator Based on Nanoparticle Magnetic Fluids. IEEE Photonics Journal, 2012, 4, 1140-1146.	2.0	28
75	Miniature In Vivo Chitosan Diaphragm-Based Fiber-Optic Ultrasound Sensor. IEEE Journal of Selected Topics in Quantum Electronics, 2012, 18, 1042-1049.	2.9	13
76	Layer-By-Layer (Chitosan/Polystyrene Sulfonate) Membrane-Based Fabry–Perot Interferometric Fiber Optic Biosensor. IEEE Journal of Selected Topics in Quantum Electronics, 2012, 18, 1457-1464.	2.9	26
77	Magneto-optical fiber sensor based on bandgap effect of photonic crystal fiber infiltrated with magnetic fluid. Applied Physics Letters, 2012, 101, .	3.3	137
78	Polyvinyl alcohol coated photonic crystal optical fiber sensor for humidity measurement. Sensors and Actuators B: Chemical, 2012, 174, 563-569.	7.8	130
79	Photonic Bandgap Fiber for Infiltration-Free Refractive-Index Sensing. IEEE Journal of Selected Topics in Quantum Electronics, 2012, 18, 1560-1565.	2.9	1
80	Magneto-optical fiber sensor based on magnetic fluid. Optics Letters, 2012, 37, 398.	3.3	162
81	Metal-enhanced fluorescence in liposomes for photothermal studies. , 2012, , .		Ο
82	Chitosan based fiber-optic Fabry–Perot humidity sensor. Sensors and Actuators B: Chemical, 2012, 169, 167-172.	7.8	219
83	Chitosan-Coated Polarization Maintaining Fiber-Based Sagnac Interferometer for Relative Humidity Measurement. IEEE Journal of Selected Topics in Quantum Electronics, 2012, 18, 1597-1604.	2.9	38
84	Simultaneous strain and temperature measurement based on a photonic crystal fiber modal-interference interacting with a long period fiber grating. Optics Communications, 2012, 285, 4874-4877.	2.1	27
85	Miniature Single-Mode Fiber Refractive Index Interferometer Sensor Based on High Order Cladding Mode and Core-Offset. IEEE Photonics Technology Letters, 2012, 24, 359-361.	2.5	20
86	Humidity Sensor Based on a Multimode-Fiber Taper Coated With Polyvinyl Alcohol Interacting With a Fiber Bragg Grating. IEEE Sensors Journal, 2012, 12, 2205-2208.	4.7	62
87	Fiber bragg gratingâ€based load sensor without temperature dependence. Microwave and Optical Technology Letters, 2012, 54, 930-933.	1.4	2
88	Temperature Sensing Based on Ethanol-Filled Photonic Crystal Fiber Modal Interferometer. IEEE Sensors Journal, 2012, 12, 2593-2597.	4.7	39
89	Cavity ringdown refractive index sensor using photonic crystal fiber interferometer. Sensors and Actuators B: Chemical, 2012, 161, 108-113.	7.8	44
90	Photonic crystal fiber refractive index sensor based on a fiber Bragg grating demodulation. Sensors and Actuators B: Chemical, 2012, 166-167, 761-765.	7.8	33

#	Article	IF	CITATIONS
91	Photonic Crystal Fiber Strain Sensor Based on Modified Mach–Zehnder Interferometer. IEEE Photonics Journal, 2012, 4, 114-118.	2.0	77
92	Temperature-Insensitive Magnetic Field Sensor Based on Nanoparticle Magnetic Fluid and Photonic Crystal Fiber. IEEE Photonics Journal, 2012, 4, 491-498.	2.0	133
93	Mach–Zehnder Photonic Crystal Interferometer in Cavity Ring-Down Loop for Curvature Measurement. IEEE Photonics Technology Letters, 2011, 23, 795-797.	2.5	31
94	Temperature Effect of Liquid Crystal in Photonic Bandgap Fiber-based Sagnac Loop. IEEE Sensors Journal, 2011, , .	4.7	0
95	A Temperature-Insensitive Twist Sensor by Using Low-Birefringence Photonic-Crystal-Fiber-Based Sagnac Interferometer. IEEE Photonics Technology Letters, 2011, 23, 920-922.	2.5	107
96	Highly sensitive fiber loop ringdown strain sensor using photonic crystal fiber interferometer. Applied Optics, 2011, 50, 3087.	2.1	43
97	Magneto-optic fiber Sagnac modulator based on magnetic fluids. Optics Letters, 2011, 36, 1425.	3.3	77
98	Highly sensitive miniature photonic crystal fiber refractive index sensor based on mode field excitation. Optics Letters, 2011, 36, 1731.	3.3	34
99	Partially liquid-filled hollow-core photonic crystal fiber polarizer. Optics Letters, 2011, 36, 3296.	3.3	54
100	Power-Referenced Optical Fiber Refractometer Based on a Hybrid Fiber Grating. IEEE Photonics Technology Letters, 2011, 23, 1706-1708.	2.5	26
101	Transversal-force sensor based on supercontinuum generation in photonic crystal fibers. Proceedings of SPIE, 2011, , .	0.8	0
102	Compact fiber bending sensor based on superimposed gratings. Proceedings of SPIE, 2011, , .	0.8	0
103	In-line fiber Mach-Zehnder interferometer combining with fiber Bragg grating for simultaneous curvature and temperature measurement. Proceedings of SPIE, 2011, , .	0.8	2
104	Photonic crystal fiber strain sensor based on cascaded Mach-Zehnder interferometer. , 2011, , .		0
105	Photonic crystal fiber integrated microfluidic chip for highly sensitive real-time chemical sensing. Proceedings of SPIE, 2011, , .	0.8	2
106	Compact photonic crystal fiber refractometer based on modal interference. Proceedings of SPIE, 2011,	0.8	1
107	Temperature-insensitive 2D tilt sensor with two chirped fiber Bragg gratings. Proceedings of SPIE, 2011, , .	0.8	1
108	Simultaneous measurement of curvature and temperature based on PCF-based interferometer and fiber Bragg grating. Optics Communications, 2011, 284, 5669-5672.	2.1	86

#	Article	IF	CITATIONS
109	Plasmonic enhanced fluorescence spectroscopy using side-polished microstructured optical fiber. Sensors and Actuators B: Chemical, 2011, 160, 196-201.	7.8	19
110	Compact refractometer based on extrinsic-phase-shift fiber Bragg grating. Sensors and Actuators A: Physical, 2011, 168, 46-50.	4.1	17
111	Refractive index measurement by using multimode interference. , 2011, , .		4
112	CLEO [®] /europe-EQEC 2011 layer-by-layer (Chitosan/ Polysodium 4-styrenesulfonate) membrane-based fiber optic sensor. , 2011, , .		0
113	Polyvinyl alcohol–coated hybrid fiber grating for relative humidity sensing. Journal of Biomedical Optics, 2011, 16, 077001.	2.6	73
114	Miniature refractometer based on modal interference in a hollow-core photonic crystal fiber with collapsed splicing. Journal of Biomedical Optics, 2011, 16, 017004.	2.6	25
115	A novel magnetic field fiber sensor by using magnetic fluid in Sagnac loop. Proceedings of SPIE, 2011, , .	0.8	10
116	Fabrication of a temperature-insensitive transverse mechanical load sensor by using a photonic crystal fiber-based Sagnac loop. Measurement Science and Technology, 2011, 22, 025204.	2.6	28
117	Fiber loop ringdown strain sensor with photonic crystal fiber based Mach-Zehnder interferometer. Proceedings of SPIE, 2011, , .	0.8	0
118	Dispersion properties of liquid photonic crystal fiber. , 2010, , .		0
119	Temperature-insensitive FBG tilt sensor with a large measurement range. Optics Communications, 2010, 283, 968-970.	2.1	55
120	Mechanically induced long-period fiber grating in side-hole single-mode fiber for temperature and refractive sensing. Optics Communications, 2010, 283, 1303-1306.	2.1	25
121	Temperature-insensitive accelerometer based on a strain-chirped FBG. Sensors and Actuators A: Physical, 2010, 157, 15-18.	4.1	45
122	Simultaneous measurement of force and temperature based on a half corroded FBG. Microwave and Optical Technology Letters, 2010, 52, 2020-2023.	1.4	14
123	Temperatureâ€independent vibration sensor with a fiber Bragg grating. Microwave and Optical Technology Letters, 2010, 52, 2282-2285.	1.4	29
124	Enhancement of temperature measurement by using photonic bandgap effect. Sensors and Actuators A: Physical, 2010, 157, 276-279.	4.1	7
125	Cavity ring-down long period grating pressure sensor. Sensors and Actuators A: Physical, 2010, 158, 207-211.	4.1	31
126	High performance chitosan diaphragm-based fiber-optic acoustic sensor. Sensors and Actuators A: Physical, 2010, 163, 42-47.	4.1	92

#	Article	IF	CITATIONS
127	Curvature measurement by using low-birefringence photonic crystal fiber based Sagnac loop. Optics Communications, 2010, 283, 3142-3144.	2.1	73
128	Temperature-insensitive 2D tilt sensor with three fiber Bragg gratings. Measurement Science and Technology, 2010, 21, 025203.	2.6	32
129	Temperature sensor based on a pressure-induced birefringent single-mode fiber loop mirror. Measurement Science and Technology, 2010, 21, 065204.	2.6	23
130	Temperature-Insensitive 2-D Pendulum Clinometer Using Two Fiber Bragg Gratings. IEEE Photonics Technology Letters, 2010, 22, 863-865.	2.5	34
131	Strain Sensor Realized by Using Low-Birefringence Photonic-Crystal-Fiber-Based Sagnac Loop. IEEE Photonics Technology Letters, 2010, 22, 1238-1240.	2.5	55
132	Sagnac interferometer based on low-birefringence photonic crystal fiber for strain measurement. , 2010, , .		0
133	Curvature sensor based on low-birefringence photonic crystal fiber Sagnac loop. , 2010, , .		1
134	Identification and measurement of gas mixture by using the support vector regression technique. Measurement Science and Technology, 2009, 20, 115601.	2.6	1
135	Sampled longâ€period fiber grating filters with narrow stop bands. Microwave and Optical Technology Letters, 2009, 51, 2401-2403.	1.4	6
136	Temperature-independent bending sensor with tilted fiber Bragg grating interacting with multimode fiber. Optics Communications, 2009, 282, 3905-3907.	2.1	87
137	Diode end-pumped passively Q-switched Nd:YAG ceramic laser with Cr4+:YAG saturable absorber. Laser Physics, 2008, 18, 1508-1511.	1.2	15
138	Fiber Cavity Ring-Down Refractive Index Sensor. IEEE Photonics Technology Letters, 2008, 20, 1351-1353.	2.5	64
139	Experimental analysis of spectral characteristics of antiresonant guiding photonic crystal fibers. Optics Letters, 2008, 33, 809.	3.3	3
140	An Enhanced SOA-Based Double-Loop Optical Buffer for Storage of Variable-Length Packet. Journal of Lightwave Technology, 2008, 26, 425-431.	4.6	17
141	Computerized automation of wavelet based denoising method to reduce speckle noise in OCT images. , 2008, , .		8
142	Analysis of hollow-core photonic bandgap fibers for evanescent wave biosensing. Journal of Biomedical Optics, 2008, 13, 054048.	2.6	11
143	Enhancing the measurement accuracy of a cavity-enhanced fiber chemical sensor by an adaptive filter. Measurement Science and Technology, 2008, 19, 115203.	2.6	18

An evolutionary algorithm to automate noise reduction in MR images. , 2008, , .

CHI CHIU CHAN

#	ARTICLE	IF	CITATIONS
145	Application of an artificial neural network for simultaneous measurement of temperature and strain by using a photonic crystal fiber long-period grating. Measurement Science and Technology, 2007, 18, 2943-2948.	2.6	12
146	A Differential Evolution Approach to PET Image De-noising. Annual International Conference of the IEEE Engineering in Medicine and Biology Society, 2007, 2007, 4173-6.	0.5	3
147	Refractive index measurement using a photonic crystal fiber. Optical Engineering, 2007, 46, 014402.	1.0	1
148	High-efficiency 1040 and 1078 nm laser emission of a Yb:Y_2O_3 ceramic laser with 976 nm diode pumping. Optics Letters, 2007, 32, 247.	3.3	64
149	Effect of liquid crystal alignment on bandgap formation in photonic bandgap fibers. Optics Letters, 2007, 32, 1989.	3.3	21
150	Temperature-tuning optical parametric oscillator based on periodically poled <inline-formula><math altimg="none" display="inline" overflow="scroll"><mrow><mi>MgO</mi><mo>:</mo><msub><mi>LiNbO</mi><mn>3</mn></msub></mrow> Optical Engineering, 2007, 46, 014205.</math </inline-formula>	10<br <	/infine-formul
151	High-resolution photonic bandgap fiber-based biochemical sensor. Journal of Biomedical Optics, 2007, 12, 044022.	2.6	13
152	Cavity ring-down long-period fibre grating strain sensor. Measurement Science and Technology, 2007, 18, 3135-3138.	2.6	24
153	Analysis of photonic crystal fibers infiltrated with nematic liquid crystal. Optics Communications, 2007, 278, 66-70.	2.1	13
154	Broad-band EDFA gain flattening by using an embedded long-period fiber grating filter. Optics Communications, 2007, 271, 377-381.	2.1	14
155	Photonic bandgap fiber for refractive index measurement. Sensors and Actuators B: Chemical, 2007, 128, 46-50.	7.8	57
156	Application of an artificial neural network for simultaneous measurement of bending curvature and temperature with long period fiber gratings. Sensors and Actuators A: Physical, 2007, 137, 262-267.	4.1	30
157	Soliton polarization dynamics in fiber lasers passively mode-locked by the nonlinear polarization rotation technique. Physical Review E, 2006, 74, 046605.	2.1	53
158	FSR-tunable fabry-Pe/spl acute/rot filter with superimposed chirped fiber Bragg gratings. IEEE Photonics Technology Letters, 2006, 18, 184-186.	2.5	11
159	Wavelength detection in FBG sensor network using tree search DMS-PSO. IEEE Photonics Technology Letters, 2006, 18, 1305-1307.	2.5	37
160	Multiwavelength Raman fiber laser with a continuously-tunable spacing. Optics Express, 2006, 14, 3288.	3.4	81
161	Investigation of photonic-crystal-fiber-based long-period gratings with aqueous solution inclusions. , 2006, , .		0
162	Bragg wavelength detection in fiber Bragg grating sensor by combining nonlinear least squares with		0

Kalman smoothing. , 2006, 6379, 30.

#	Article	IF	CITATIONS
163	Application of support vector machine for trace gas detection by using temperature-tuning optical parametric oscillator. , 2006, , .		0
164	Tunable photonic band gaps in a photonic crystal fiber. , 2006, , .		0
165	Trace-gas detection based on the temperature-tuning periodically poled MgO: LiNbO 3 optical parametric oscillator. , 2006, 6379, 39.		0
166	Bandwidth-tunable filter and spacing-tunable comb filter with chirped-fiber Bragg gratings. Optics Communications, 2006, 259, 645-648.	2.1	29
167	Embedded long-period fiber grating bending sensor. Sensors and Actuators A: Physical, 2006, 125, 267-272.	4.1	18
168	Wavelength-selective all-fiber filter based on a single long-period fiber grating and a misaligned splicing point. Optics Communications, 2006, 258, 159-163.	2.1	52
169	Improving the measurement accuracy of CRD fibre amplified loop gas sensing system by using a digital LMS adaptive filter. Measurement Science and Technology, 2006, 17, 2349-2354.	2.6	28
170	Enhancement of the measurement range of FBG sensors in a WDM network: a self-organizing network solution. Sensors and Actuators A: Physical, 2005, 118, 233-237.	4.1	5
171	High relative humidity measurements using gelatin coated long-period grating sensors. Sensors and Actuators B: Chemical, 2005, 110, 335-341.	7.8	113
172	High relative humidity sensing using gelatin-coated long period grating. , 2005, 5855, 375.		8
173	Tunable WDM filter with 0.8-nm channel spacing using a pair of long-period fiber gratings. IEEE Photonics Technology Letters, 2005, 17, 795-797.	2.5	18
174	Temperature-insensitive tilt sensor with strain-chirped fiber Bragg gratings. IEEE Photonics Technology Letters, 2005, 17, 2394-2396.	2.5	73
175	Tunable WDM filters based on cascaded long-period fiber gratings. , 2005, , .		1
176	A bandwidth-tunable FBG filter with fixed center wavelength. Microwave and Optical Technology Letters, 2004, 41, 22-24.	1.4	18
177	A high-resolution tunable fiber Bragg grating filter. Microwave and Optical Technology Letters, 2004, 42, 89-92.	1.4	3
178	Humidity sensing using plastic optical fibers. Microwave and Optical Technology Letters, 2004, 43, 387-390.	1.4	16
179	Improving the Performance of FBG Sensors in a WDM Network Using a Simulated Annealing Technique. IEEE Photonics Technology Letters, 2004, 16, 227-229.	2.5	15
180	Noise Limit in Heterodyne Interferometer Demodulator for FBG-Based Sensors. Journal of Lightwave Technology, 2004, 22, 2287-2295.	4.6	8

#	Article	IF	CITATIONS
181	Humidity sensing using plastic optical fibers. , 2004, 5590, 77.		2
182	Noise limit in heterodyne interferometer demodulator for FBG based sensors. , 2004, , .		0
183	Bending measurement using embedded long-period fiber gratings. , 2004, , .		1
184	High-resolution tunable fiber Bragg grating filter. , 2004, , .		1
185	Novel fiber Bragg grating sensor for temperature-insensitive displacement measurement. , 2004, , .		0
186	Simultaneous measurement of curvature and temperature for LPG bending sensor. , 2004, , .		4
187	Intrinsic crosstalk analysis of a serial TDM FGB sensor array by using a tunable laser. Microwave and Optical Technology Letters, 2003, 36, 2-4.	1.4	24
188	Enhancement of the measurement range of FBG sensors in a WDM network using a minimum variance shift technique coupled with amplitude-wavelength dual coding. Optics Communications, 2003, 215, 289-294.	2.1	10
189	Improving measurement accuracy of fiber Bragg grating sensor using digital matched filter. Sensors and Actuators A: Physical, 2003, 104, 19-24.	4.1	15
190	Improving the performance of a FBG sensor network using a genetic algorithm. Sensors and Actuators A: Physical, 2003, 107, 57-61.	4.1	53
191	Improving the wavelength detection accuracy of FBG sensors using an ADALINE network. IEEE Photonics Technology Letters, 2003, 15, 1126-1128.	2.5	25
192	A largely tunable CFBG-based dispersion compensator with fixed center wavelength. Optics Express, 2003, 11, 2970.	3.4	61
193	Effects of active fiber length on the tunability of erbium-doped fiber ring lasers. Optics Express, 2003, 11, 3622.	3.4	26
194	Cantilever optical vibrometer using fiber Bragg grating. Optical Engineering, 2003, 42, 3179.	1.0	28
195	Fiber Bragg grating current sensor using linear magnetic actuator. Optical Engineering, 2002, 41, 557.	1.0	11
196	Simultaneous interrogation of multiple FBG sensors for dynamic measurands. , 2002, , .		1
197	A novel wavelength detection technique for fiber Bragg grating sensors. IEEE Photonics Technology Letters, 2002, 14, 678-680.	2.5	60
198	Magneto-mechanical tuning of fiber Bragg grating filter. Microwave and Optical Technology Letters, 2002, 33, 73-74.	1.4	4

#	Article	IF	CITATIONS
199	Experimental investigation of a 4-FBG TDM sensor array with a tunable laser source. Microwave and Optical Technology Letters, 2002, 33, 435-437.	1.4	4
200	A fiber Bragg grating sensor for static and dynamic measurands. Sensors and Actuators A: Physical, 2002, 96, 21-24.	4.1	27
201	Time division multiplexed strain sensing system by the use of dual-wavelength fiber Bragg gratings. Sensors and Actuators A: Physical, 2002, 100, 175-179.	4.1	2
202	Enhancement of wavelength detection accuracy in fiber Bragg grating sensors by using a spectrum correlation technique. Optics Communications, 2002, 212, 29-33.	2.1	35
203	<title>Performance of a time-division-multiplexed fiber Bragg grating sensor array with a tunable
laser source</title> . , 2001, , .		0
204	Fiber Bragg grating sensor for static and dynamic measurands. , 2001, 4596, 119.		0
205	Characterization of crosstalk of a TDM FBG sensor array using a laser source. Optics and Laser Technology, 2001, 33, 299-304.	4.6	13
206	Strain monitoring in composite-strengthened concrete structures using optical fibre sensors. Composites Part B: Engineering, 2001, 32, 33-45.	12.0	61
207	Investigation of unwanted interferometric signals in a fiber Bragg grating sensor using a tunable laser and a first derivative interrogation technique. Optics Communications, 2000, 173, 203-210.	2.1	18
208	Recent progress of white light interferometric fiberoptic strain sensing techniques. Review of Scientific Instruments, 2000, 71, 4648.	1.3	19
209	Performance analysis of a time-division-multiplexed fiber Bragg grating sensor array by use of a tunable laser source. IEEE Journal of Selected Topics in Quantum Electronics, 2000, 6, 741-749.	2.9	44
210	Experimental demonstration of a fiber-optic gas sensor network addressed by FMCW. IEEE Photonics Technology Letters, 2000, 12, 1546-1548.	2.5	15
211	Enhancement of measurement accuracy in fiber Bragg grating sensors by using digital signal processing. Optics and Laser Technology, 1999, 31, 299-307.	4.6	40
212	Comparative studies of three adaptive controllers. ISA Transactions, 1999, 38, 43-53.	5.7	11
213	Simultaneous measurement of temperature and strain: an artificial neural network approach. IEEE Photonics Technology Letters, 1998, 10, 854-856.	2.5	17
214	<title>Effect of interferometric noise in fiber Bragg grating sensors using tunable laser sources</title> . , 1998, 3330, 272.		0
215	Comparison of GPC Controller and a Pid Auto-Tuner for a Heating Plant. International Journal of Electrical Engineering and Education, 1997, 34, 316-325.	0.8	0
216	<title>Simultaneous recovery of temperature and strain: an artificial neural network
approach</title> ., 1997, 3099, 362.		0

#	Article	IF	CITATIONS
217	WITHIN-DAY AND BETWEEN-DAY RELIABILITY OF A FBG-BASED SMART SOCK SYSTEM FOR MEASURING ACTIVE TOE FLEXION DISPLACEMENT OF THE HALLUX. Journal of Mechanics in Medicine and Biology, 0, , 2150057.	0.7	0